كليـــــة الهنـــد ســـــة
المطرية بالقاهرة

مجلـــة البحـــوث الهنـــدسيـــة

مجلـــد ٨١ يونيـــه ٢٠٠٢

INVESTIGATION OF FILM CONDENSATION OF R-11 IN INTERNALLY GROOVED HORIZONTAL TUBES

A. M. Osman, Eed A. Abdel-Hadi and Sherif H. Taher
Mechanical Engineering Department, Shobra Faculty of Engineering, Zagazig University

ABSTRACT

Enhancement of heat transfer coefficient has a great attractive attention in the present time due to its importance for many thermal and engineering applications. The objective of the present investigation was to experimentally determine the heat transfer coefficient during condensation of R-11 inside internally grooved tubes. The experimental measurements are carried out at saturation temperatures between 30°C and 50°C, heat flux up to 10 kW/m^2 and Reynolds number varies from $3x10^3$ to 10^5. Helical grooves of three different shapes, rectangular, trapezoidal and rectangular with rounded corners, axial pitch varied from 25 mm to 70 mm and groove depth varied from 0.3mm to 0.9 mm are tested. An experimental apparatus was designed and constructed here for this purpose. The condensing heat transfer coefficient is correlated with these parameters. The results obtained here compare favourably with the available published data.

KEY WORDS: Heat transfer coefficient, condensation, helical grooves, axial pitch, groove depth and shape.

NOMENCLATURE

A_i	inside surface area of the condensing tube	m^2
A_o	outside surface area of the condensing tube	m^2
D_i	condensing tube inner diameter	m
D_o	condensing tube outer diameter	m
d	groove depth	mm
c	specific heat	kJ/kg K
h	convective heat transfer coefficient	W/m^2 K
h_{fg}	latent heat of vaporization or condensation	kJ/kg
k	thermal conductivity	W/m K
L	condensing tube length	m
LMTD	logarithmic mean temperature difference	°C
m	mass flow rate	kg/s
Nu	Nusselt number	$h_{ref} D_i/k_{ref}$
P	pressure	bar
Q	heat transfer rate	W
q	heat flux	W/m^2
Re	Reynolds number for the refrigerant vapor	$4m/(\pi D_i \mu_v)$

S	axial pitch	mm
T	temperature	K
U	overall heat transfer coefficient	$W/m^2 K$

Greek

μ	viscosity	$N s/m^2$

Subscripts

c	condenser
in	inlet to the test section
m	mean
o	outside surface
out	outlet from the test section
ref	refrigerant
S	for different axial pitch
S,d	for different axial pitch and different depth
sm	smooth surface
v	vapor
w	water

INTRODUCTION

Condensation inside horizontal tubes is widely used in many thermal applications such as refrigeration and air conditioning equipment. The analysis of heat transfer in such systems is extremely important for the design of condensers. Most of the existing investigations deal with the condensation process on smooth surface. Very few studies are available concerning the effect of enhancing the condensing surface of the condenser tubes.

Experimental study for the condensation process has been performed by Graham, et al. [1] covering a range of 75-450 kg/m^2s mass velocity in an 8.91 mm inside diameter, axially grooved, micro-fin tube using R-134a. At 75 kg/m^2s the axially grooved tubes performed marginally better than the smooth tube. Mass velocity of 150 kg/m^2s and higher in axially grooved tube performed significantly better than both smooth and helically grooved tubes. Pressure drop characteristics of the axially grooved tubes are similar to those found with using an 18° helical grooves.

Chiang [2] found that axially grooved tubes in general show higher performance than helical grooved tubes over a wide range of mass velocities and vapor qualities during condensation. Direct comparison between the axially grooved tubes and an 18° helical grooved tubes could not be made because the grooves were of significantly different fin geometries and fin frequencies.

Local heat transfer and pressure drop measurements were obtained during condensation of R-11 in horizontal micro-fin tubes by Nozu et al. [3]. A smooth tube and two micro-fin tubes with different fin dimensions were tested. Flow observations with the use of an industrial bore-scope revealed that the condensate swirled along the grooves and a thick condensate film covered the fins in the lower part of the tube in the low quality region. Static pressure gradients in the micro-fin tubes were 70% larger than that in a smooth tube.

A method was presented by Nozu and Honda [4] to estimate the condensing heat transfer coefficient in horizontal spirally grooved micro-fin tubes. Based on the study performed for flow observation, a laminar film condensation model in the annular flow regime was proposed. The model assumed that the condensate flow occurs through the grooves. The condensate film is segmented into thin and thick film regions. In the thin film region formed on the fin surface, the condensate is assumed to be drained by the combined surface tension and vapor shear forces. In the thick film region formed in the grooves, on the other hand, the condensate assumed to be driven by the vapor shear force. Data for local heat transfer were obtained using four fluids (R-11, R-22, R-123 and R-134a) and three micro-fin tubes where the results agreed with the available predictions within 15.1% deviation.

Cavallini et al. [5] measured the heat transfer coefficient and pressure drop during condensation inside tubes when operating with pure refrigerants (R134a, R125, R32, R236ea) and the nearly azeotropic refrigerant R410A. Data were taken also for condensation of R-22 and reported for reference. The effect of vapor quality, mass velocity, saturation temperature and temperature difference between saturation and tube wall on the heat transfer coefficient were investigated.

Boissieux et al. [6] presented results for the local heat transfer coefficient obtained during condensation of Isceon 59, R407C and R404A in a smooth horizontal tube. The results have been compared with the available correlations for the condensation process to assess the validity of the proposed models.

Liu [7] investigated experimentally the condensing heat transfer coefficient and pressure drop characteristics of R-134a and R-22, flowing inside a 9.5 mm diameter axially grooved, to obtain quasi-local heat transfer correlations. When comparing R-22 for the same refrigerant flow rate, the condensing heat transfer coefficients for R-134a was 8% to 18% higher, but with 50% higher in pressure drop.

A semi-empirical model was proposed, by Yang and Webb [8], to predict the condensation heat transfer coefficient inside small hydraulic diameter extruded aluminum tubes having microgrooves. The model accounts for the effects of vapor shear and surface tension forces. The vapor shear model was based on the use of an equivalent mass velocity and the heat transfer analogy.

Local heat transfer and pressure drop measurements were made, by Nozu et al. [9], during condensation of a nonazeotropic refrigerant mixture R114/R113 in the annuli of horizontal double tube condensers. The inner tube was a 19.1 mm outside diameter with copper wire fins soldered on the outer surface. The heat transfer coefficient based on the bulk vapor to wall temperature difference was found to be considerably smaller for R114/R113 mixture than for pure R113. An empirical equation for the vapor phase mass transfer coefficient was derived, in which the dimensionless parameters were introduced on the basis of the published results for turbulent single phase flow in smooth and rough tubes with and without surface tension. The measured condensing heat transfer coefficient for R114/R113 mixture was correlated with the proposed model and 14.3% deviation was found.

A mathematical model of annular film condensation in a mini tube has been developed by Begg et al. [10]. In this model the liquid flow has been coupled with the vapor flow along the liquid-vapor interface through the interfacial temperature, heat flux, shear stress, and pressure jump conditions due to surface tension effects. The model predicts

the shape of the liquid-vapor interface along the condenser and the length of the two phase flow region. The numerical results show that complete condensation of the incoming vapor is possible at comparatively low heat loads. Observations from a flow visualization experiment of water vapor condensing in a horizontal glass tube confirm the existence of annular film condensation leading to the complete condensation phenomenon in small diameter (<3.5 mm) circular tubes.

From the above analysis for the existing literature concerned with the condensing heat transfer coefficient, it can be concluded that there is still more investigations are needed in particular those related to the enhancement of the condensing surface of condenser tubes from the geometrical aspects and operating conditions view points.

The objective of the present study is to extend the previous investigations performed to enhance the condensing surface especially those having internal grooves. The heat transfer characteristics during condensation of R-11 vapor flowing inside grooved condenser tubes is studied. The refrigerant R-11 is chosen here as a representative for the available and cheapest refrigerants. The measured data are used to deduce empirical correlations for the condensing heat transfer coefficient as a function of the proposed geometrical modification made on the internal surface of the condensing tube. In order to obtain these correlations, experimental measurements have been performed on smooth and grooved tubes. The results obtained from the smooth tube are compared with the corresponding available published results. Also correlations are introduced for the experimental measurements performed here.

EXPERIMENTAL APPARATUS

Figure 1 shows a schematic diagram of the experimental apparatus designed and constructed in the present investigation to study the condensing heat transfer coefficient of R-11. The vapor generated in an electrically heated evaporator (6) flows through a soft copper tube to a condensing tube (10). The vapor condenses in the condensing tube, and the condensate flows through a control valve, and returns downward by gravity to the evaporator as the condenser has a slope of 30 mm every one meter of its length. The outer tube (11) has 75 mm inner diameter and made of galvanized steel inside which cooling water is flowing. The evaporator has a sight glass (5) for observation to ensure a minimum liquid level of 200 mm above the electric heater (7). The condenser is covered with a cylindrical glass wool insulation (12) of 25.4 mm thickness and wrapped outside with aluminum foil to minimize the radial heat loss. The refrigerant is coming from the charging line (1) through a control valve (2). A pressure cutout (3) and pressure gage (4) are connected to the refrigerant circuit. The aim of the pressure cutout is to separate the electric power line from the apparatus if the pressure raised above a certain value. The cooling water flows counter currently to the flow of refrigerant, which is chosen here for better heat exchange in comparison with parallel flow, using water tank (13) and water pump (16). The water circuit is provided with an electric heater (17) to keep the temperature of the cooling water constant at a chosen value to avoid subcooling of the refrigerant, thermostat (18), ball valve (19) and flow meter (20). The test section as indicated in Fig. 2 is a horizontal double tube condenser where the refrigerant (R-11) flows in the inner tube and the cooling water flows counter-currently in the outer annulus. Nine similar copper tubes having same length, inner and outer diameters are used. These tubes have

internal helical grooves of different axial pitch, depth and shape. Each tube has 19 mm inner diameter, 22.3 mm outer diameter and 2 m length and has two ends flare to facilitate its changing. Each condensing tube was manufactured in segments, each segment is of 200 mm length grooved separately and then assembled together using copper sleeves and soldered. To avoid deflection of the condensing tube, three teflon rods fitted through three holes drilled on the outer tube at the middle length for this purpose and in the same time to keep the condensing tube concentric with the outer tube. Copper-constantan thermocouples of 0.3 mm diameter are used with multi-meter having an accuracy of 0.1°C. Five thermocouples as shown in Fig. 2 are fixed on the outer surface of the condensing tube which are embedded at a depth of 0.5 mm with good contact with the tube surface. Three additional thermocouples are fixed inside the condensing tube to measure the temperature of the refrigerant. The different shapes and the physical dimensions of the grooves are given in Fig. 3a. Figure 3b shows the helical shape of the groove and its axial pitch. The photograph given in Fig. 4 shows the different components of the experimental apparatus used in the present study.

EXPERIMENTAL PROCEDURE

After assembling the condenser the air in the system was drawn by a vacuum pump, and fresh refrigerant R-11 was sucked into the condenser copper tube until the circuit is filled with enough amount of the refrigerant showing a level of 200 mm at least above the electric heater. The power is supplied to the heater according to the required heat flux and the cooling water is allowed to flow in the annular section. After steady-state conditions has been reached (within 30 minutes), the following variables are measured:

i) the outer surface temperatures of the condensing tube at five locations shown in Fig. 2.
ii) the refrigerant temperatures, at three locations, Fig. 2.
iii) refrigerant pressure.
iv) cooling water temperatures.
v) cooling water flow rate.
vi) electrical power.

Condensation has been confirmed by allowing 0.5 °C for refrigerant outlet temperature to be less than the saturation conditions and keep it fixed by adjusting the cooling water flow rate. Table (1) gives the different parameters and test conditions used in the experimental runs performed in the present investigation.

Table (1): Parameters and test conditions of the experimental runs

Parameter	Operating conditions
Heat flux, W/m^2	From 2900 to 10000
Reynolds number	From $3x10^3$ to 10^5
Refrigerant pressure, bar	1.25, 1.75 and 2.357
Groove shape	Rectangular, trapezoidal, and rectangular with rounded corners
Axial pitch, mm	25, 40, 55 and 70
Groove depth, mm	0.3, 0.6 and 0.9

HEAT TRANSFER CALCULATIONS

The following equations have been employed to calculate the heat transfer coefficient of refrigerant from the experimental measurements recorded here at steady state conditions.

The heat transfer rate in the condenser can be determined from the heat balance of the cooling water:

$$Q_c = m_w \cdot c_w \cdot (T_{w,out} - T_{w,in}) \quad (1)$$

The refrigerant mass flow rate was calculated from the energy balance of the system for complete condensation. The refrigerant properties were taken at saturation conditions in the condenser [11.

$$m_{ref} = Q_c / h_{fg} \quad (2)$$

The overall heat transfer coefficient based on the outside surface area of the condensing tube is as follows:

$$U_o = Q_c / (A_o \, LMTD) \quad (3)$$

Where, LMTD is the logarithmic mean temperature difference based on the inlet and outlet temperatures of cooling water and refrigerant.

The heat transfer coefficient of the cooling water side is calculated as:

$$h_w = Q_c / [A_o \cdot (T_o - T_{m,w})] \quad (4)$$

Where, T_o : average temperature of the outside surface of the condensing tube.
$T_{m,w}$: the mean temperature of the cooling water:

$$T_{m,w} = (T_{w,in} + T_{w,out}) / 2 \quad (5)$$

The refrigerant side heat transfer coefficient, h_{ref} was obtained as [7]:

$$(1/h_{ref}) = (1/U_o) - A_i/(A_o \cdot h_w) - A_i \ln(D_o/D_i)/(2\pi kL) \quad (6)$$

As the circulation of refrigerant is done naturally, in addition that the mass velocities used here are small, accordingly, no pressure drop is noticed as its value is too low to be measured by the available devices. Hence the pressure drop in this study is neglected.

RESULTS AND DISUSSION

An experimental apparatus has been constructed here to determine the condensing heat transfer coefficient of R-11 as a representative for the available and cheapest refrigerants. The measurements are used to deduce correlations for condensing heat transfer coefficient using smooth and internally grooved condensing tubes. Figures 5 shows the variation of the condensing heat transfer coefficient for smooth tube with

the heat flux for different refrigerant pressures. It can be noticed that the condensing heat transfer coefficient increases with the increase of heat flux. For the same heat flux the heat transfer coefficient increases with the increase of refrigerant pressure. The variation of Nusselt number with the Reynolds number (calculated for R-11 as vapor at inlet conditions of the condensing tube [12]) at different refrigerant pressures is depicted in Fig. 6. As expected the Nusselt number increases with the increase in Reynolds number. For the same Reynolds number as the refrigerant pressure increases the Nusselt number increases.

A correlation is deduced here for the condensing heat transfer coefficient as a function of the heat flux, q and the refrigerant pressure, P for the data presented in Fig. 5. This correlation is given by:

$$h_{sm} = a\ q^{b} \qquad \text{for} \quad 1.25 \text{ bar} \le P \le 2.357 \text{ bar}, \quad 2900 \text{ W} \le q \le 10000 \text{ W} \qquad (7)$$

where: $a = 0.023\ P^2 - 0.0286$

$b = (\ 0.578 / P^{1.5}\ ) + 0.99$

where, h_{sm} is the condensing heat transfer coefficient for smooth tube.

Figure 7 shows a comparison between the measured and correlated heat transfer coefficients. The correlation fits the measured data with a maximum deviation of ±5% for the mentioned operating conditions.

To assess validity of the present results, the condensing heat transfer coefficient is compared with the published data. For the lake of corresponding results for R-11, the present results are compared with the available ones. Figure 8 compares the present results with those obtained by Shao and Granryd [13]. The experimental measurements compare favourably with the published data.

In the following part the effect of using helical grooves inside the condensing tube on the condensing heat transfer coefficient is presented. The study includes helical grooves of different shapes as shown in Fig. 3a with different axial pitch (25, 40, 55 and 70 mm, Fig. 3b) and of different depth (0.3, 0.6 and 0.9 mm) keeping same surface area for all grooves.

To determine the suitable groove shape the condensing heat transfer coefficient is calculated for different shapes namely, rectangular, trapezoidal and rectangular with rounded corners. Figure 9 indicates the variation of the condensing heat transfer coefficient with the heat flux for different groove shapes. It is clear that the condensing heat transfer coefficient increases with the increase in heat flux for all groove shapes. For the same heat flux, the condensing heat transfer coefficient for rectangular grooves is relatively higher than the trapezoidal and rectangular with rounded corners. Figure 10 gives a relation between Nusselt number and Reynolds number for different groove shapes and the given test conditions. Again for rectangular groove shape, the Nusselt number has its highest value compared with the other two shapes for all values of Reynolds number. This is due to the large contact length of the groove root and the expected enhancement in turbulence due to the sharp corners of the rectangular shape.

Accordingly the grooves of rectangular shape are considered in all cases subjected to the different geometrical and operating conditions studied here.

Figure 11 shows the variation of the condensing heat transfer coefficient with the heat flux for different refrigerant pressures using helical internal grooves of rectangular shape with 0.6 mm depth and 55 mm axial pitch as a case study. It is observed that with the increase in heat flux the condensing heat transfer coefficient increases.

Figure 12 depicts the variation of the Nusselt number with the Reynolds number for different refrigerant pressures and the indicated test conditions. For the same pressure, the Nusselt number increases for any increase in Reynolds number. The highest Nusselt number occurs at the highest refrigerant pressure. Also, the condensing heat transfer coefficient is calculated from the present experimental data using condensing tube of different axial pitch (25, 40, 55 and 70 mm). Figure 13 shows the variation of the condensing heat transfer coefficient with the heat flux for different axial pitch. For the same heat flux, decreasing the axial pitch makes better contact of the liquid film of the refrigerant with the inner tube wall and helps the liquid to move faster which transports more energy and enhances the condensing heat transfer coefficient.

Figure 14 presents a relation between Nusselt number and Reynolds number for different axial pitch and the given test conditions. For the same Reynolds number, the Nusselt number increases with the decrease in axial pitch.

The enhancement of the condensing heat transfer coefficient due to change of axial pitch of the grooved tube is indicated in Fig. 15. It is obvious that as the axial pitch increases the condensing heat transfer coefficient decreases. The enhancement ratio in the condensing heat transfer coefficient ($h_{ref,S}/h_{sm}$) is 2.41 at S/D_i=1.316, while this ratio is 1.4 at S/D_i=3.684 in comparison with smooth tube.

The results plotted for different axial pitch in Fig. 13 are used to correlate the condensing heat transfer coefficient with the axial pitch (S) and the inside diameter of the condenser tube (D_i) for rectangular shape. This correlation is as follows:

$$h_{ref,S}/h_{sm} = 3.3522/\sqrt{(S/Di)} - 0.3634 \qquad 25\ mm \leq S \leq 70\ mm \qquad (8)$$

D_i is the inner diameter of the condensing tube in mm. and $h_{ref,S}$ is the condensing heat transfer coefficient with variable axial pitch.

Figure 16 shows a comparison between the measured and correlated results given by equation (8) for grooves of rectangular shape. The correlation fits the measured data within ±9% max deviation for the given test conditions.

The variation of the condensing heat transfer coefficient with the heat flux for different groove depth is depicted in Fig. 17. For the same heat flux the condensing heat transfer coefficient increases with the increase of groove depth.

Figure 18 presents the variation of the Nusselt number with the Reynolds number for different groove depth. The use of grooves of any depth causes a noticeable increase in Nusselt number compared with smooth tube. For the same Reynolds number as the groove depth increases more improvement in Nusselt number is obtained.

The condensing heat transfer coefficient is correlated with the groove axial pitch (S), inside diameter of condensing tube (D_i) and the groove depth (d) for rectangular groove shape. The resulting correlation is given as follows:

$$h_{ref,S,d} / h_{sm} = [3.3522/\sqrt{(S/Di)} - 0.3634]/[\ 1.0649 - 11.289(d/\ D_i)^{1.5}\ ]$$

for $0.3\ mm \leq d \leq 0.9\ mm$ (depth)
$25\ mm \leq S \leq 70\ mm$ (pitch) (9)

where, $h_{ref,S,d}$ is the condensing heat transfer coefficient of variable axial pitch and groove depth.and h_{sm} is calculated from equation (7).
Fig. 19 indicates the change in the enhancement ratio of the condensing heat transfer coefficient ($h_{ref,S,d}$ / h_{sm}) due to change of groove depth. It is clear that the enhancement ratio increases with the increase in the groove depth. At d/D_i=0.016 the enhancement ratio is 2.45, while at d/D_i=0.047 this ratio is 2.7 in comparison with smooth tube. For the range of test conditions used here the variation in the condensing heat transfer coefficient becomes almost constant after d/D_i=0.03.
Figure 20 shows that the correlation given by equation (9) fits the measured results for the mentioned test conditions with ±9% maximum deviation.

CONCLUSIONS

Experimental measurements have been performed here during condensation of R-11 in horizontal copper tube provided with helical grooves generated on its internal surface. Correlations for calculating the condensing heat transfer coefficient has been proposed based on the present experimental measurements. From the above analysis the following conclusions are obtained:

1- The refrigerant heat transfer coefficient for smooth tube is significantly increased with the increase of both the heat flux and the refrigerant pressure.
2- A correlation for the condensing heat transfer coefficient for smooth tube using R-11 as the working fluid is obtained which fits equation (7) within ±5% maximum deviation for the present test conditions.
3- The condensing heat transfer coefficient for the condensing tube is increased with:
   (i) Using grooves of rectangular shape.
   (ii) Decreasing of the axial pitch, which gives enhancement ratio up to 2.41 compared with smooth tube.
   (iii) Increasing the groove depth, which results in increasing the enhancement ratio up to 2.7, compared with smooth tube.

A general correlation for the condensing heat transfer coefficient is deduced as function of the axial pitch and groove depth, which fits the experimental measurements with ±9% maximum deviation.

REFERENCES

1. D. Graham, J. C. Chato and T. A. Newell; "Heat Transfer and Pressure Drop During Condensation of Refrigerant 134a in an Axially Grooved Tube", International Journal of Heat and Mass Transfer, Vol. 42, pp. 1935-1944, 1999.
2. R. Chiang; "Heat Transfer and Pressure Drop During Evaporation and Condensation of Refrigerant-22 in 7.5 mm and 10 mm Diameter Axial and Helical

Grooved Tubes"; AIChE Heat Transfer Symposium, Atlanta, 89(295), pp. 205-210, 1993.

3. S. Nozu., H. Katayama, H. Nakata and H. Honda; "Condensation of Refrigerant CFC11 in Horizontal Microfin Tubes Proposal of a Correlation Equation for Frictional Pressure Gradient", Experimental Thermal Fluid Science, Vol. 18, No. 1, pp. 82-96,. 1998.
4. S. Nozu and H. Honda; "Condensation of Refrigerants in Horizontal, Spirally Grooved Micro-fin Tubes: Numerical Analysis of Heat Transfer in the Annular Flow Regime"; ASME; Journal of Heat Transfer, Vol. 122; pp. 80-91; 2000.
5. A. Cavallini, G. Censi, D. Del Col, L. Doretti, G. A. Longo and L. Rossetto; "Experimental Investigation on Condensation Heat Transfer and Pressure Drop of New HFC Refrigerants (R134a, R125, R32, R410A, R236ea) in a Horizontal Smooth Tube"; International Journal of Refrigeration; 24; pp. 73-87; 2001.
6. X. Boissieux, M. R. Heikal and R. A. Johns;" Two-phase Heat Transfer Coefficients of Three HFC Refrigerants Inside a Horizontal Smooth Tube, Part II: Condensation"; International Journal of Refrigeration; 23; pp. 345-352; 2000.
7. X. Liu; " Condensing and Evaporating Heat Transfer and Pressure Drop Characteristics of HFC-134a and HCFC-22"; ASME; Journal of Heat Transfer; Vol. 119; pp. 158-163; 1997.
8. C. Y. Yang and R. L. Webb; " A Predictive Model for Condensation in Small Hydraulic Diameter Tubes Having Axial micro-fins"; ASME, Journal of Heat Transfer Vol. 119; pp. 776-782; 1997.
9. S. Nozu, K. Ozaki and H. Inaba and H. Honda, " Condensation of a Nonazeotropic Refrigerant Mixture R114/R113 in Horizontal Annuli with an Enhanced Inner Tube"; ASME; Journal of Heat Transfer; Vol. 114; pp. 201-209; 1992.
10. E. Begg, D. Khrustalev and A. Faghri;" Complete Condensation of Forced Convection Two Phase Flow in a Miniature Tube"; ASME; Journal of Heat Transfer; Vol. 121; pp. 904-915; 1999.
11. American Society of Heating, Refrigerating and Air Conditioning Engineers, ASHRAE; Handbook of Fundamentals; 1981.
12. F. P. Incropera and D. P. DeWitt, Fundamentals of Heat Transfer, John Wiley & Sons, 1981.
13. D. W. Shao and E. Granryd;" Experimental and Theoretical Study on Flow Condensation with Non-azeotropic Refrigerant Mixtures of R32/R134a"; International Journal of Refrigeration; Vol. 21; No.3; pp. 230-246; 1998.

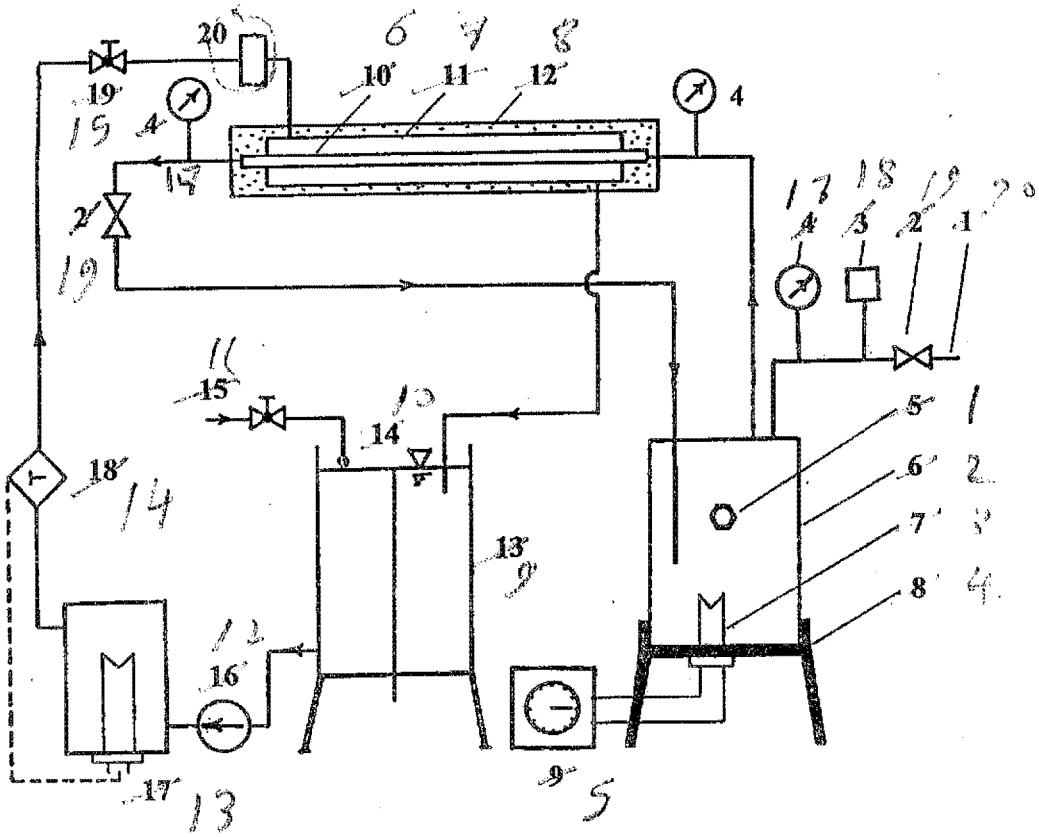

1. Charging line
2. Gate valve
3. Pressure cut-out
4. Pressure gauge
5. Sight glass
6. Evaporator
7. Electric heater
8. Frame
9. Power regulator
10. Test tube
11. Water tube (annulus)
12. Thermal insulation
13. Water tank
14. Over-flow
15. Water supply
16. Water pump
17. Water heater
18. Thermostat
19. Ball valve
20. Flow-meter

Fig. 1 Experimental apparatus layout

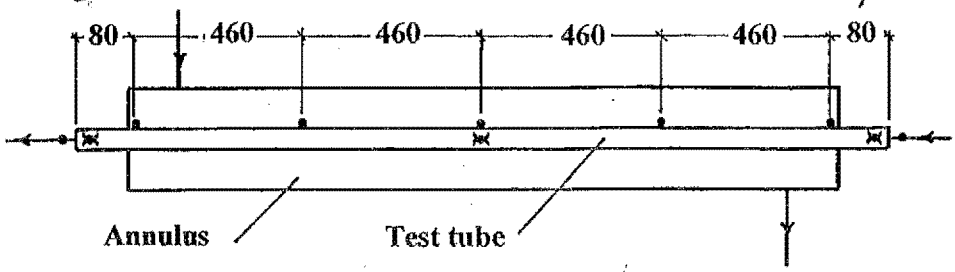

Thermocouples locations

- outside surface of condensing tube
- inside the condensing tube

Dim. in mm

Fig. 2 Test section and thermocouple locations

Depth mm	Rectangular shape	Trapezoidal shape	Rounded corners shape
0.3	2.1		
0.6	1.5	2.0	1.8
0.9	0.9		

Scale 10:1

Fig. 3.a Dimensions of different shapes of the internal groove

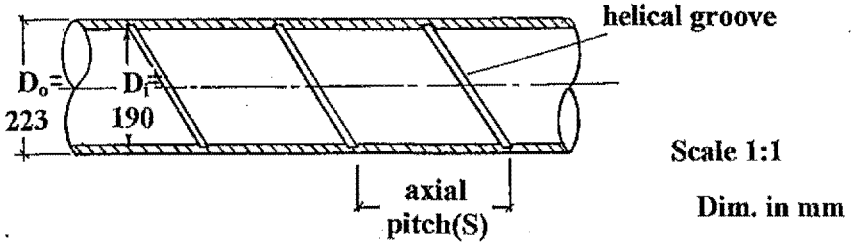

Scale 1:1

Dim. in mm

Fig. 3.b Dimensions of the axial pitch

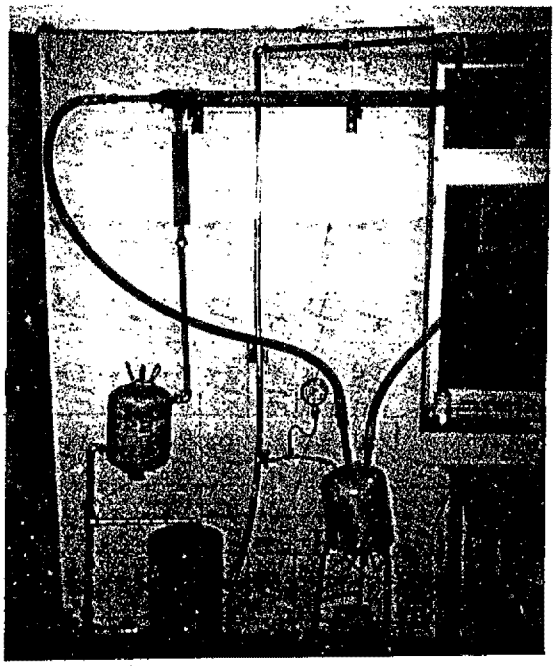

Fig. 4 Photograph of the experimental apparatus

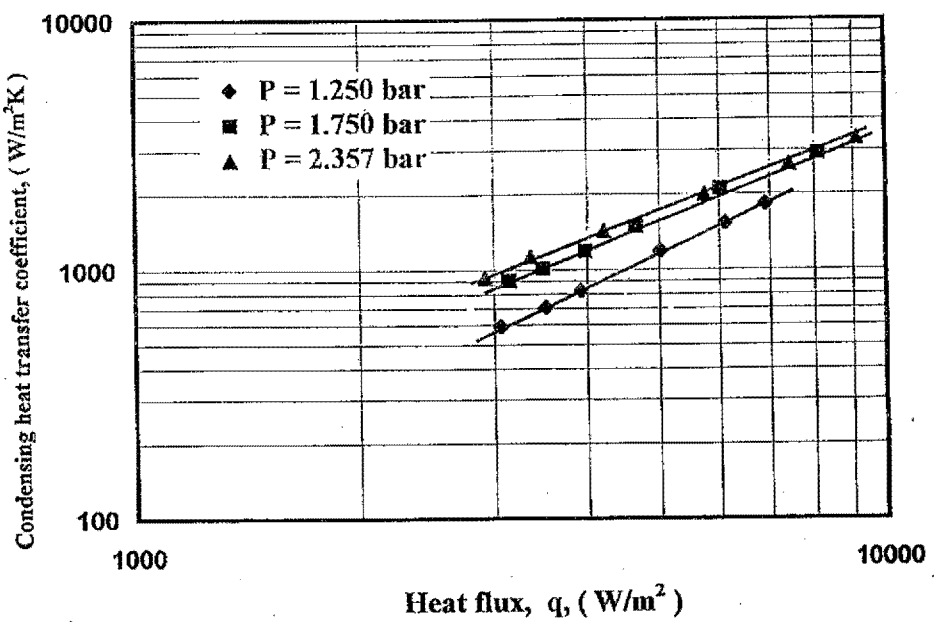

Fig. 5 Variation of the condensing heat transfer coefficient with heat flux for smooth tube at different pressures

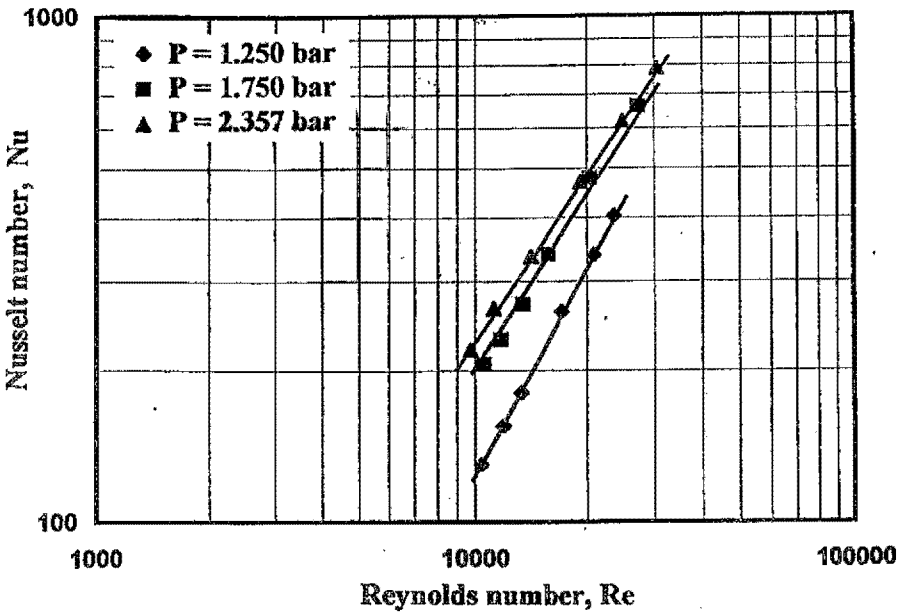

Fig. 6 Variation of Nusselt number with Reynolds number for smooth tube at different pressures

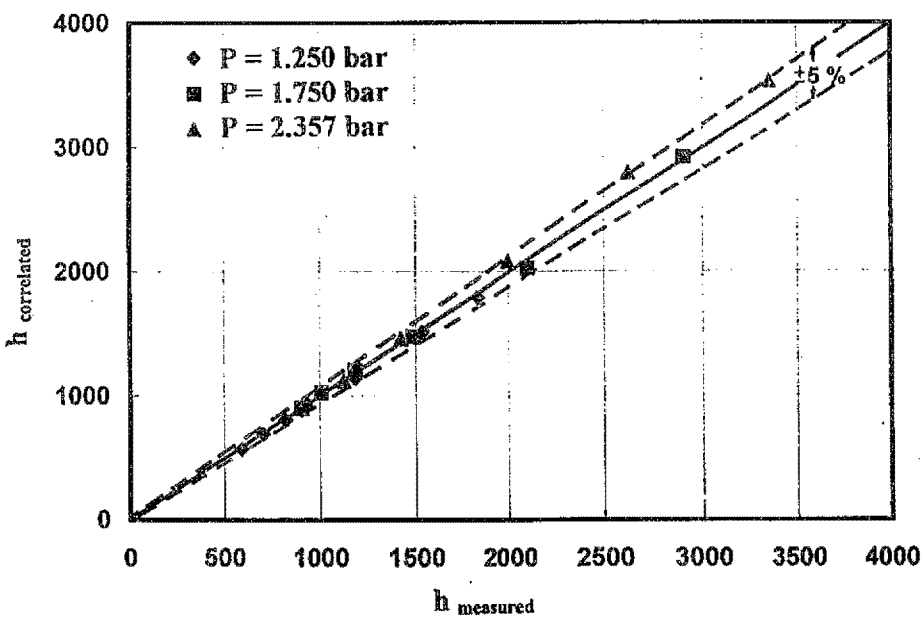

Fig. 7 Comparison between the experimental and correlated results (Eq. 7) for smooth tube

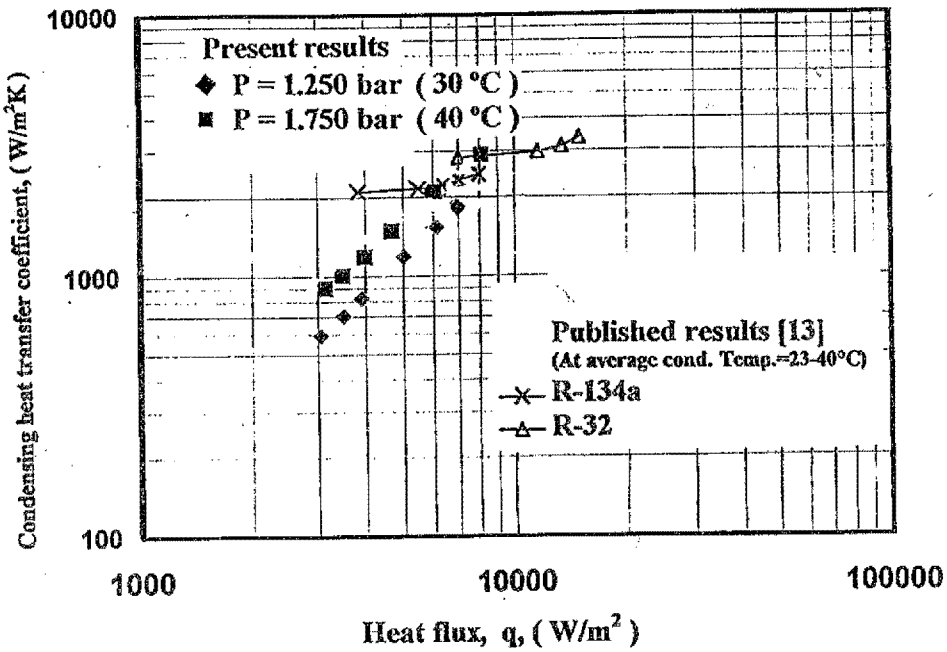

Fig. 8 Variation of the condensing heat transfer coefficient with the heat flux for the present results and published data [13]

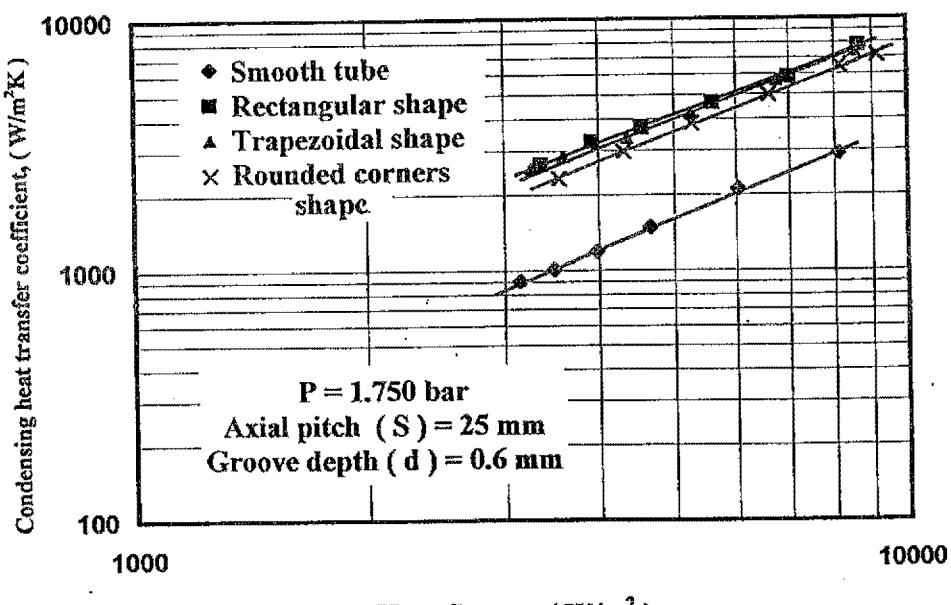

Fig. 9 Variation of the condensing heat transfer coefficient with heat flux for different groove shapes

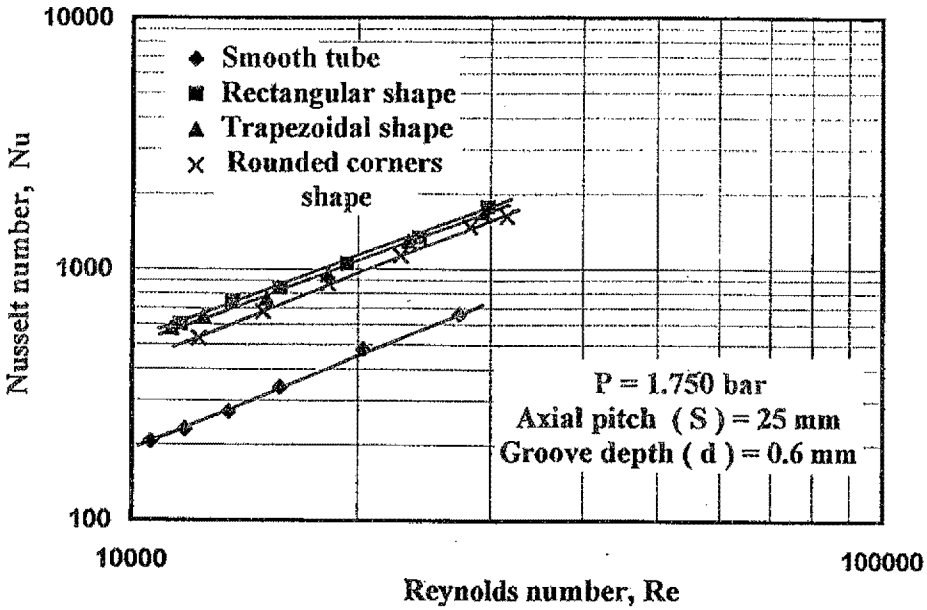

Fig. 10 Variation of Nusselt number with Reynolds number for different groove shapes

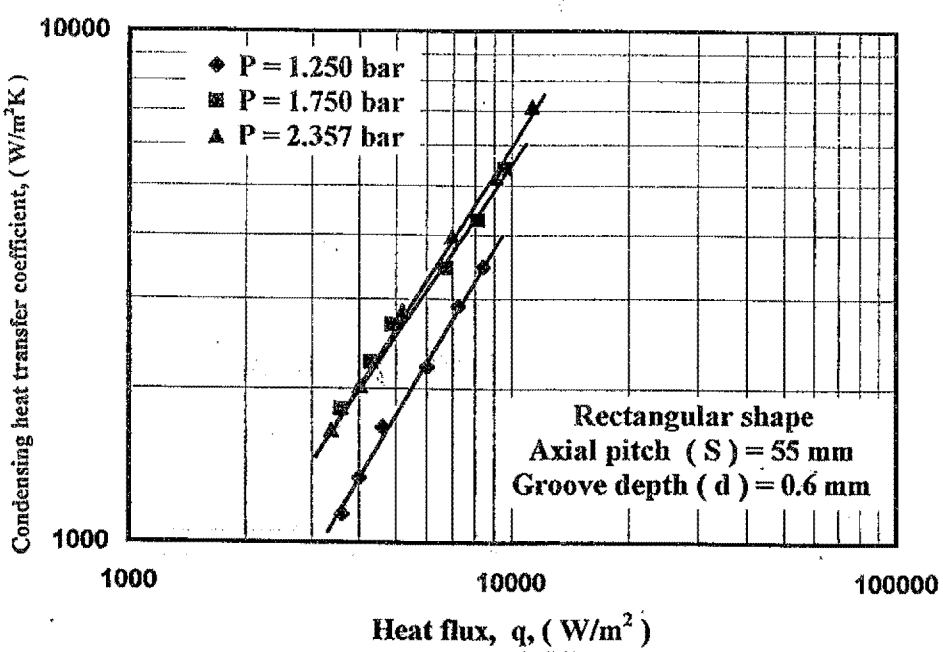

Fig. 11 Variation of the condensing heat transfer coefficient with heat flux for different pressures

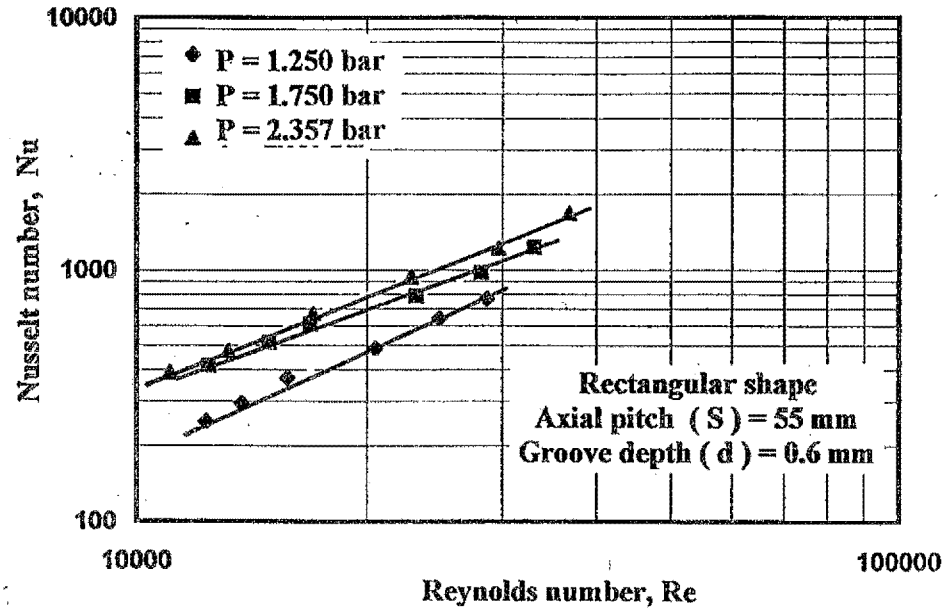

Fig. 12 Variation of Nusselt number with Reynolds number for different pressures

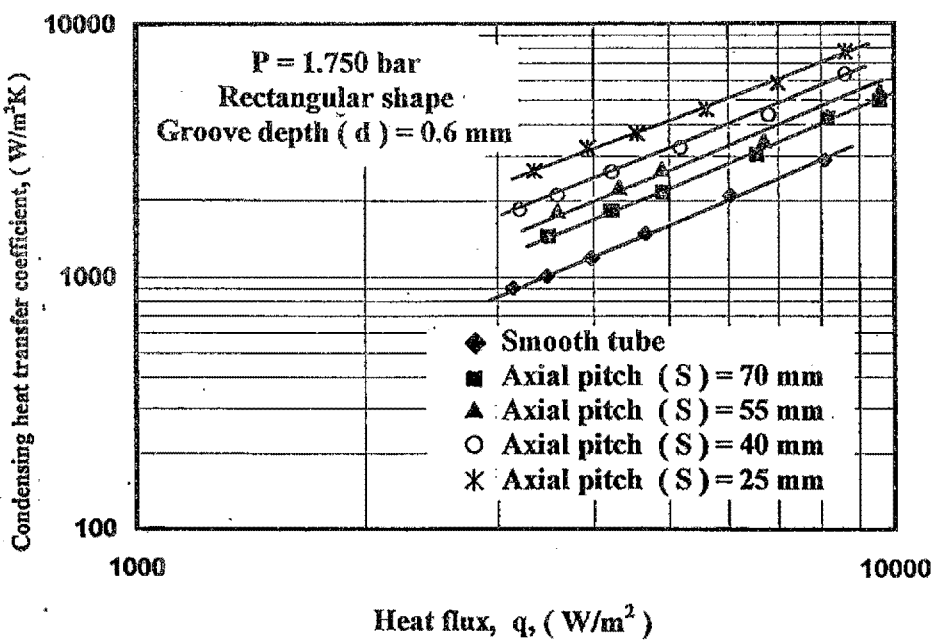

Fig. 13 Variation of the condensing heat transfer coefficient with heat flux for different axial pitch

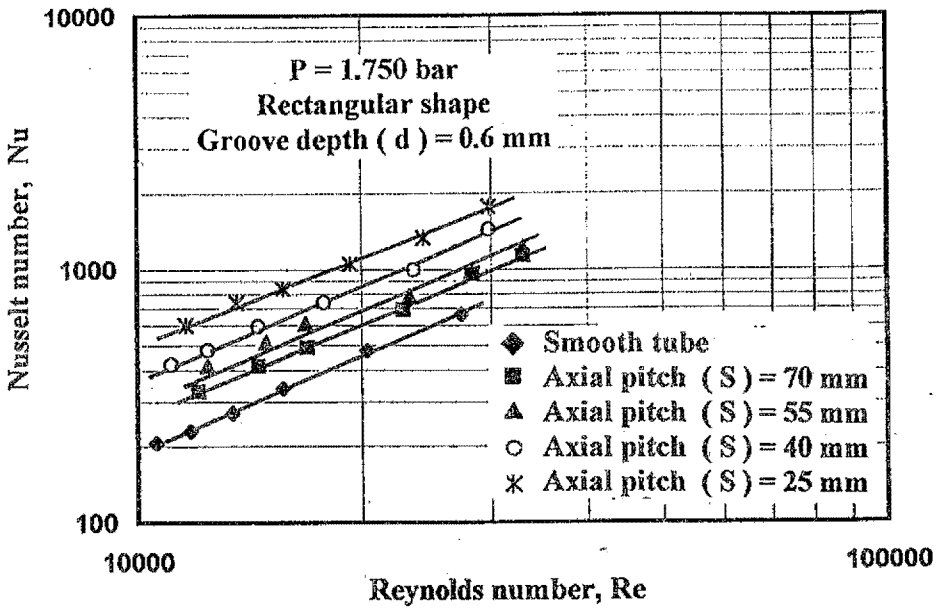

Fig. 14 Variation of Nusselt number with Reynolds number for different axial pitch

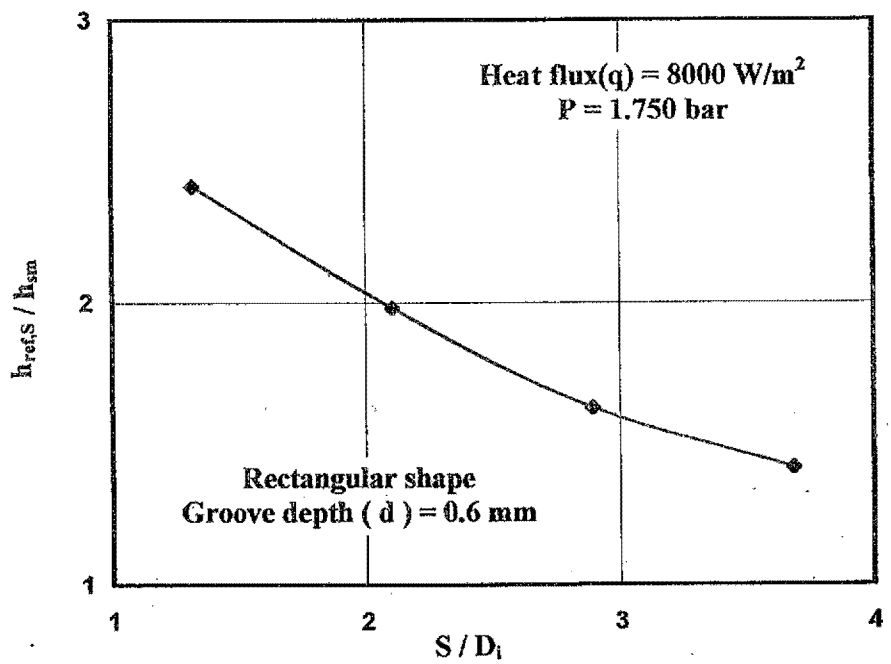

Fig. 15 Enhancement of condensing heat transfer coefficient due to change in axial pitch

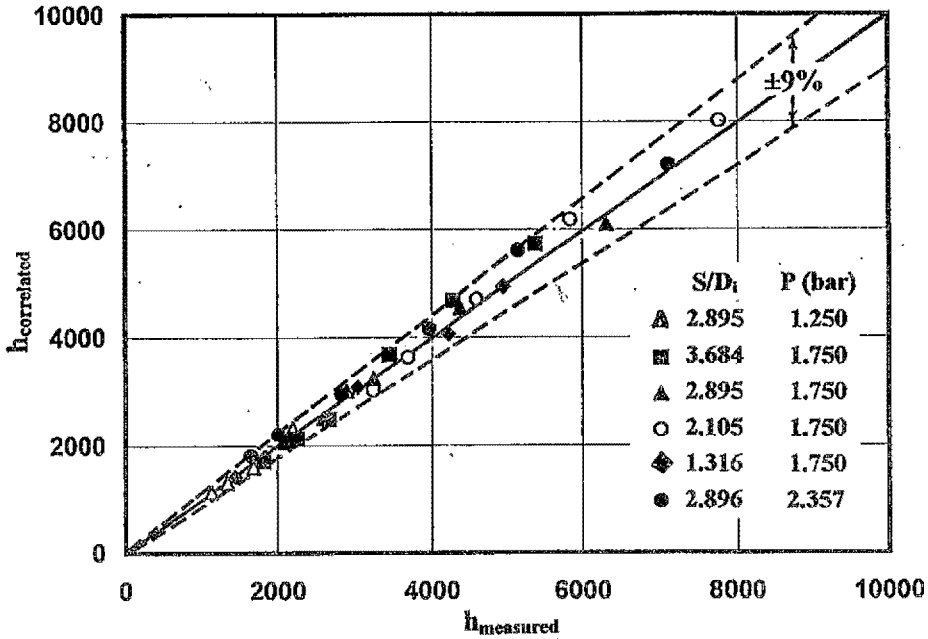

Fig. 16 Comparison between the experimental condensing heat transfer coefficient and the correlated results (Eq. 8)

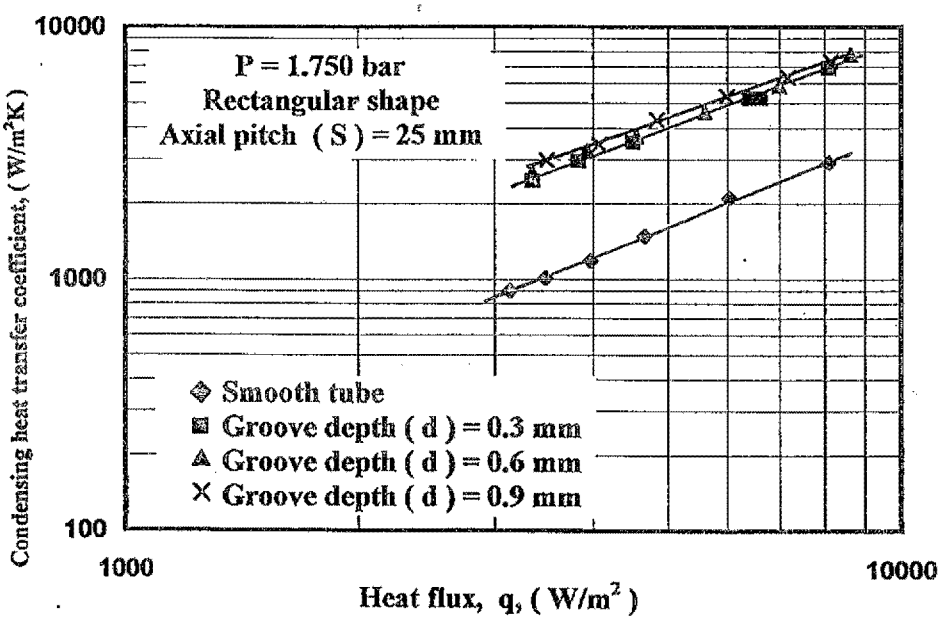

Fig. 17 Variation of the condensing heat transfer coefficient with heat flux for different groove depth

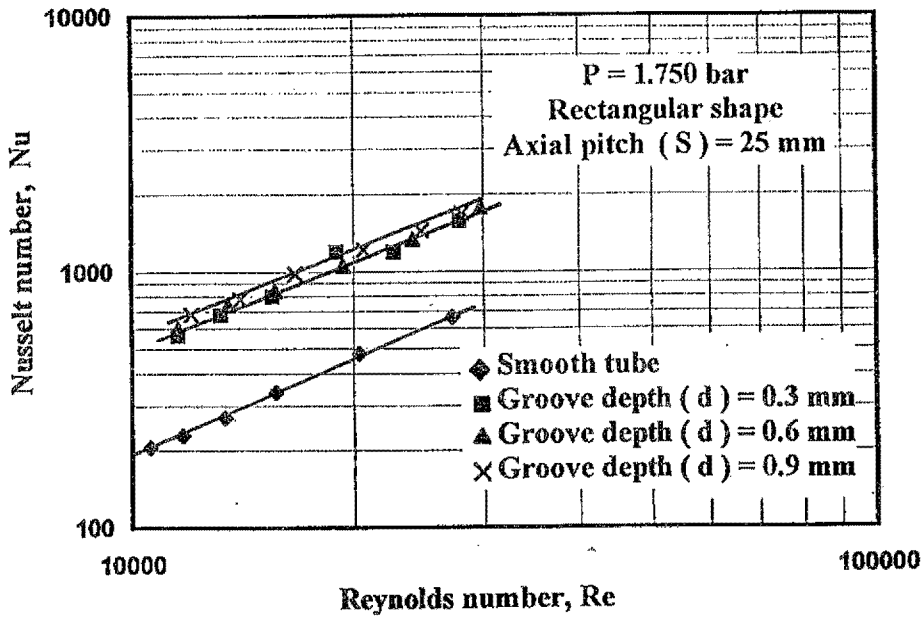

Fig. 18 Variation of Nusselt number with Reynolds number flux for different groove depth

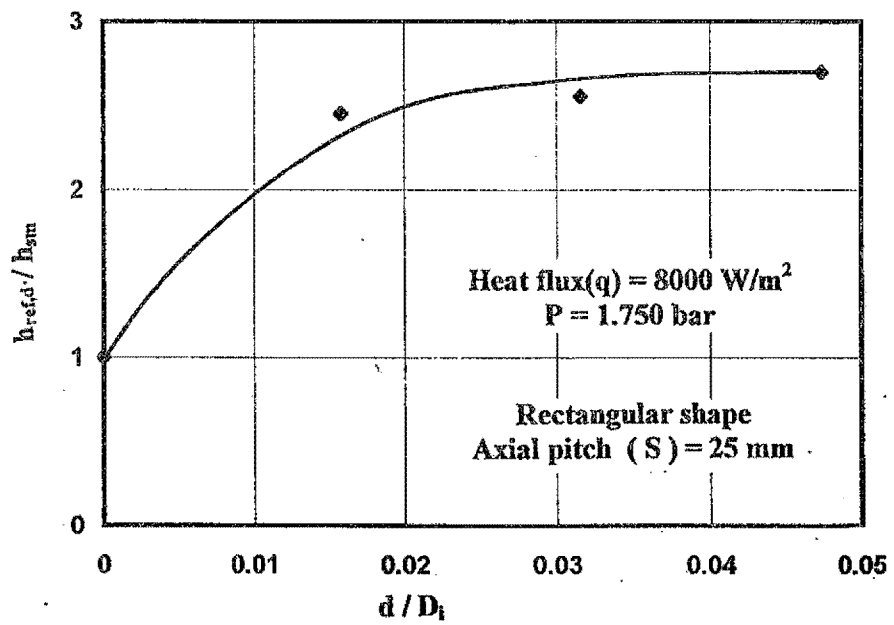

Fig. 19 Enhancement of condensing heat transfer coefficient due to change in groove depth

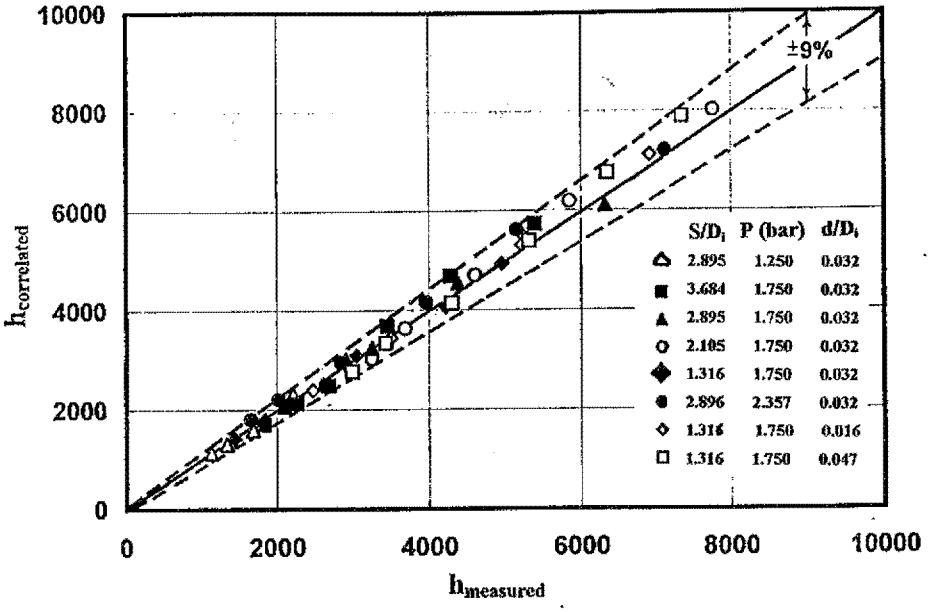

Fig. 20 Comparison between the experimental condensing heat transfer coefficient and the correlated results (Eq. 9)